Article (refereed) - postprint

Strong, Rebecca J.; Halsall, Crispin J.; Jones, Kevin C.; Shore, Richard F.; Martin, Francis L. 2016. **Infrared spectroscopy detects changes in an amphibian cell line induced by fungicides: comparison of single and mixture effects**.

Contact CEH NORA team at
noraceh@ceh.ac.uk

Infrared spectroscopy detects changes in an amphibian cell line induced by fungicides: comparison of single and mixture effects

Rebecca J. Strong[1], Crispin J. Halsall[1*], Kevin C. Jones[1], Richard F. Shore[2] and Francis L. Martin[1,3*]

[1]*Lancaster Environment Centre, Lancaster University, Bailrigg, Lancaster LA1 4YQ, UK*

[2] *Centre for Ecology and Hydrology, Lancaster University, Bailrigg, Lancaster LA1 4YQ, UK*

[3]*School of Pharmacy and Biomedical Sciences, University of Central Lancashire, Preston PR1 2HE, UK*

[*] **Corresponding authors.** Email address: c.halsall@lancaster.ac.uk (C.J. Halsall);

f.martin@lancaster.ac.uk (F.L. Martin)

Highlights

- IR spectroscopy applied to analyse the *Xenopus laevis* (A6) cell line
- Effects of low concentrations of carbendazim or flusilazole determined
- Alterations identified following single or binary exposures
- A sensitive technique for examining environmentally-relevant levels of fungicides
- A6 cells could be a useful model to identify agents that threaten amphibian health

Abstract

Amphibians are regarded as sensitive sentinels of environmental pollution due to their

permeable skin and complex life cycle, which usually involves reproduction and development

in the aquatic environment. Fungicides are widely applied agrochemicals and have been associated with developmental defects in amphibians; thus, it is important to determine chronic effects of environmentally-relevant concentrations of such contaminants in target cells. Infrared (IR) spectroscopy has been employed to signature the biological effects of environmental contaminants through extracting key features in IR spectra with chemometric methods. Herein, the *Xenopus laevis* (A6) cell line was exposed to low concentrations of carbendazim (a benzimidazole fungicide) or flusilazole (a triazole fungicide) either singly or as a binary mixture. Cells were then examined using attenuated total reflection Fourier-transform IR (ATR-FTIR) spectroscopy coupled with multivariate analysis. Results indicate significant changes in the IR spectra of cells induced by both agents at all concentrations following single exposures, primarily in regions associated with protein and phospholipids. Distinct differences were apparent in the IR spectra of cells exposed to carbendazim and those exposed to flusilazole, suggesting different mechanisms of action. Exposure to binary mixtures of carbendazim and flusilazole also induced significant spectral alterations, again in regions associated with phospholipids and proteins, but also in regions associated with DNA and carbohydrates. Overall these findings demonstrate that IR spectroscopy is a sensitive technique for examining the effects of environmentally-relevant levels of fungicides at the cellular level. The combination of IR spectroscopy with the A6 cell line could serve as a useful model to identify agents that might threaten amphibian health in a rapid and high throughput manner.

Keywords: A6 cells; ATR-FTIR spectroscopy; carbendazim; flusilazole; *Xenopus laevis*

Introduction

Large declines in amphibian populations have been reported since the 1990's (Houlahan et al., 2000; Stuart et al., 2004), with environmental pollution reported as a significant factor in

these declines (Sparling et al., 2001). The life cycle of amphibians usually encompasses reproduction and early development in the aquatic environment, meaning that this group of organisms may be susceptible to run-off from agricultural sources, such as pesticide application, which is often coincident with this sensitive period of development (Hanlon and Parris, 2014; Hayes et al., 2006; Mann et al., 2009). Such factors, in addition to the permeable skin of amphibians (Quaranta et al., 2009), mean that this group is a be a sentinel organism, indicative of early deterioration in environmental quality (Sparling et al., 2010).

Fungicides are widely used in agriculture in order to prevent and treat diseases in commercial crops such as wheat and soybean (Belden et al., 2010; McMullen et al., 2012). Two classes of fungicide frequently used in agricultural practice, either singly or in combination are the benzimidazole and triazole fungicides. Benzimidazole fungicides exert their toxic effect on fungal spores through inhibition of microtubule assembly, by binding to tubulin, the major component of microtubules (Berg et al., 1986; Davidse, 1986; Wolff, 2009). Triazole fungicides, in contrast, interfere with steroid biosynthesis and therefore formation of fungal cell walls through inhibition of sterol-14α-demethylase (CYP51), an enzyme present in all eukaryotes (Bossche et al., 1995; Zarn et al., 2003). As a consequence, the structure of the plasma membrane is disrupted, making it prone to further damage (Georgopapadakou, 1998; Lorito et al., 1996). Both benzimidazole and triazole fungicides have been associated with negative effects in non-target organisms, including amphibians. Such effects include endocrine disruption in adult amphibians (Poulsen et al., 2015), and developmental defects such as craniofacial abnormalities in the case of triazole fungicides (Di Renzo et al., 2011; Groppelli et al., 2005; Papis et al., 2006), or inhibition of the differentiation of neural tissues and organ dysplasia following exposure to benzimidazole fungicides (Yoon et al., 2003; Yoon et al., 2008).

Investigating the effects of environmental pollutants at the cellular level is of importance in ecotoxicological research because the key interaction between chemical contaminants and organisms initially occurs within cells (Fent, 2001). In addition, the use of an *in vitro* cell culture model reduces the number of vertebrates used in environmental risk assessment, thus reducing ethical concerns (Scholz et al., 2013). Infrared (IR) spectroscopy is being increasingly applied in cell-based assays in order to determine molecular modifications caused by chemical stressors, based on changes in the IR absorbance spectra (Holman et al., 2000a). Exposure of a sample to IR radiation will cause the functional groups within the sample to absorb the IR radiation and vibrate in several ways, including stretching, bending and deformation. These absorptions and vibrations can then be directly correlated to biochemical molecules, with peaks in the spectrum corresponding to the chemical structure of a particular entity, *e.g.*, lipid ~ 1740 cm^{-1}, DNA ~ 1080 cm^{-1}, Amide I and II ~ 1650 and 1550 cm^{-1} respectively, thus providing a 'biomolecular fingerprint' in the form of an IR spectrum (Ellis and Goodacre, 2006; Kelly et al., 2011; Martin et al., 2010). . Previous studies have found a high concordance between traditional toxicological endpoints and those measured by FTIR spectroscopy. For example, in HEPG2 cells exposed to TCDD, there was a positive correlation between CYP1A1 expression and IR absorption of the phosphate band (Holman et al., 2000b). MCF-7 cells exposed to 17β-estradiol showed comparable EC-50 values when assessed with either the E-screen assay or FTIR spectroscopy, with the results from FTIR spectroscopy obtained in a much shorter time, a key advantage of this technique (Johnson et al., 2014). As IR spectroscopy is able to analyse lipids, carbohydrates, proteins and nucleic acids concurrently, it is valuable technique for metabolic fingerprinting (Ellis and Goodacre, 2006).

The resulting fingerprint is highly complex and information rich, comprising hundreds of features (wavenumbers), therefore multivariate techniques such as principal

component analysis (PCA) or linear discriminant analysis (LDA) are often applied in order to reduce the complexity of the data sets into a small number of factors (scores). The application of chemometric methods like PCA and LDA allows the extraction of key features from the IR spectrum in the form of loadings and cluster vectors, which denote which regions of the IR spectrum are responsible for segregation between control and treated cells when viewed alongside the scores plots (Baker et al., 2014; Martin et al., 2010; Trevisan et al., 2012). The combination of IR spectroscopy and multivariate techniques for feature extraction has previously been applied in human, algal and bacterial cell types in order to distinguish between treated and control cells and generate potential biomarkers based upon the loadings and cluster vectors generated (Heys et al., 2014; Johnson et al., 2014; Llabjani et al., 2010, 2011; Mecozzi et al., 2007; Riding et al., 2012a; Ukpebor et al., 2011).

In this study, ATR-FTIR spectroscopy coupled with multivariate feature-extraction techniques was employed in order to detect the effects of two commonly used fungicides: carbendazim, a benzimidazole fungicide, and flusilazole, a triazole-derived fungicide at low, environmentally relevant concentrations (Chatupote and Panapitukkul, 2005; Palma et al., 2004) ranging from 0.05-5 nM in A6 cells, a continuous epithelial cell line derived from the kidney of the African clawed frog, *Xenopus laevis*. A6 cells are a well characterised cell line, having previously been used in toxicity studies (Gorrochategui et al., 2016) measuring responses such as expression of heat shock proteins (HSPs), intracellular calcium and cell cycle progression after exposure to a variety of environmental contaminants (Bjerregaard, 2007; Bjerregaard et al., 2001; Darasch et al., 1988; Faurskov and Bjerregaard, 1997; Faurskov and Bjerregaard, 2000; Faurskov and Bjerregaard, 2002; Heikkila et al., 1987; Khamis and Heikkila, 2013; Music et al., 2014; Thit et al., 2013; Woolfson and Heikkila, 2009; Yu et al., 2007). Additionally, as amphibians are exposed to multiple chemical stressors in the environment (Hua and Relyea, 2014; Relyea, 2009), cells were also exposed

to mixtures of carbendazim and flusilazole. The aims of the study were as follows: **1)** To determine if ATR-FTIR spectroscopy coupled with multivariate feature-extraction techniques could detect changes induced to cellular biomolecules by carbendazim and flusilazole across a concentration range in the A6 cell line; **2)** To determine differences in the mechanism of action of each agent through direct comparison of the features extracted from their IR spectra; and, **3)** To determine the combined effects of carbendazim and flusilazole on cells in binary mixtures in comparison to single agent effects through comparison of the features extracted from their IR spectra.

Materials and Methods

Cell Culture

Xenopus laevis A6 kidney epithelial cells were purchased from Sigma Aldrich (Dorset, UK) and grown at 22°C in T75 tissue culture flasks in 70% (diluted with distilled water to adjust to amphibian osmolarity) Leibovitz's (L15) media supplemented with 10% v/v fetal bovine serum (FBS) and 1% penicillin/streptomycin (100 U/mL/100 µg/mL). Cells were routinely subcultured every 7 days by partial digestion in 0.25% trypsin-EDTA and prior to incorporation into experiments. Media was replaced every 72 h. Flasks that had reached 80-90% confluency were used for experiments. All cell culture consumables were purchased from Gibco Life Technologies (Paisley, UK) unless otherwise stated.

Test Agents

Flusilazole (product no. 45753) and carbendazim (product no. 45368) were purchased as PESTANAL® analytical standards from Sigma Aldrich (Poole, Dorset) and made up to 10 µM stocks solutions in dimethylsulfoxide (DMSO) (also from Sigma Aldrich). Serial

dilutions of the stock solutions were made to give the appropriate concentrations in the treatment flasks. Test agent/vehicle control solutions did not exceed 1% v/v in the treatment flasks.

Cell Treatments

Routinely cultured A6 cells were trypsin-disaggregated, resuspended in complete media and seeded in T25 flasks at a density of 5×10^4 cells/ml. Cells attached for 24 h before treatment with the test agents as either single concentrations or binary mixtures for a further 24 h. This treatment time is optimal for IR spectroscopy studies as it allows the recording of distinct spectral variations, whilst avoiding large amounts of damage from apoptosis and necrosis to the cells (Derenne et al., 2012). For the single concentrations, cells were treated with 5 nM, 1 nM, 0.5 nM, 0.1 nM and 0.05 nM of carbendazim or flusilazole, plus a vehicle control (DMSO). For the binary mixtures, cells were treated with 5 nM and 0.05 nM of flusilazole and carbendazim in the following combinations: 0.05 nM carbendazim, 0.05 nM flusilazole; 5 nM carbendazim, 5 nM flusilazole; 0.05 nM carbendazim, 5 nM flusilazole; 5 nM carbendazim, 0.05 nM flusilazole. Cells were treated with single concentrations of carbendazim or flusilazole (5 nM and 0.05 nM) together with an equivalent volume of DMSO in order to account for any effects of volume when comparing with the mixtures. For each treatment, nine independent replicates were carried out.

Following treatments, cells were again disaggregated and the cell suspensions immediately fixed in 70% ethanol and stored at 4°C until use. Fixed cell suspensions were transferred onto 1 cm × 1cm Low-E reflective glass slides (Kevley Technologies, Chesterland, OH, USA), dried overnight and stored in a desiccator until analysis.

ATR-FTIR Spectroscopy

Five spectra per slide were acquired using a Tensor 27 FTIR spectrometer with Helios ATR attachment (Bruker Optics Ltd, Coventry, UK) containing a diamond crystal ($\approx$250 μm $\times$ 250 μm sampling area). Spectra were acquired at 8 cm^{-1} resolution with 2$\times$ zero-filling, giving a data-spacing of 4 cm^{-1} over the range 400-4000 cm^{-1}. Distilled water was used to clean the crystal in between analysis of each sample. A new background reading was taken prior to the analysis of each sample in order to account for changes in atmospheric conditions.

Data Processing and Analysis

Single treatments

Spectra were cut at the biochemical cell fingerprint region (1800-900 cm^{-1}), baseline corrected using Savitzky-Golay 2nd order differentiation (2nd order polynomial and 9 filter coefficients), and vector normalised. Data were mean-centred before the application of PCA-LDA with leave-one-out cross-validation; this method uses a small portion of the dataset to train the model in order to prevent LDA overfitting. PCA reduces the spectra (227 wavenumbers) into a smaller number of principal components for input into LDA. In this case 14 PCs were picked for flusilazole and 15 PCs for carbendazim as this represented ~95% of the variance in the data and represented where the variance began to plateau, thus preventing noise being inputted into further analysis with LDA. LDA maximises the differences between classes and minimises the heterogeneity within classes. The data can then be viewed as scores, to determine how the different treatments separate from the control class (Trevisan et al., 2012). The wavenumbers responsible for the separation of the scores were determined using the cluster vector (CV) approach. Cluster vectors generate 'pseudo-spectra'; which have a direct relation to the original absorbance spectra and are used to reveal

biochemical alterations specific to each data class relative to the control, which is set at the origin (Trevisan et al., 2012). A peak detecting algorithm with a data-spacing of 20 cm^{-1} was then employed to select the seven most prominent wavenumbers in the CVs that contributed to the segregation between control and treated cells.

Comparison of cells treated with carbendazim *vs.* cells treated with flusilazole

In addition, a direct comparison was made of the spectral signature of cells treated with carbendazim in comparison to those treated with flusilazole. As no significant differences were found between the individual concentrations of flusilazole and carbendazim (see results) direct comparisons between these two agents were assessed by compiling spectra of all concentrations of the data. Two approaches were taken to compare cells treated with carbendazim to those with flusilazole: cross-validated PCA-LDA and forward feature selection (FFS). For both approaches, difference spectra were first calculated (following pre-processing), where the mean spectra of the vehicle control was subtracted from the mean spectra of the treated cells for each test agent giving the actual metabolic modifications caused by each test agent (Derenne et al., 2012). Cross-validated PCA-LDA was used as before, with 18 PCs incorporated into the LDA model, generating scores and a CV plot (flusilazole-treated cells at the origin) as before, with a peak detection algorithm employed as detailed previously. FFS incorporates sub-sets of wavenumbers into a dataset, ranking them based on how they contribute to the correct classification of each labelled dataset. It is a useful technique for comparison with PCA-LDA, as the biomarkers generated from this approach may be more discriminatory than those generated by PCA-LDA (Trevisan et al., 2014). This approach generates a feature selection histogram (FSH) that provides a count of the frequency (number of hits) each wavenumber was selected (Trevisan et al., 2012). The FSH was produced using a Gaussian-fit classifier with random sub-sampling, repeated 100

times to randomise training and test data (90% training, 10% data). Five variables were used to improve the stability of biomarker identification (Trevisan et al., 2014).

Comparison of binary mixtures with single treatments

Cells exposed to the combination treatments of carbendazim and flusilazole were also pre-processed as before and analysed with PCA-LDA (9-10 PCs), generating scores and loadings plots in order to pinpoint biochemical alterations induced by each binary mixture for comparison with single-agent effects.

All spectral pre-processing and data analysis was implemented using the IRootLab toolbox https://code.google.com/p/irootlab/ (Martin et al., 2010; Trevisan et al., 2013) in Matlab (r2012a) (The MathWorks, Inc., USA), unless otherwise stated.

Statistical Analysis

Scores generated from PCA-LDA were averaged to give one score per replicate (9 per treatment) and either two-sample t-tests or one-way ANOVA followed by Tukey's post-hoc tests was applied to calculate differences between the scores generated from PCA-LDA analysis. Analysis was carried out in GraphPad Prism 6 software (GraphPad Software Inc, CA, USA).

Results

Single Treatments

A representative second derivative spectrum of A6 cells in the 1800-900 cm⁻¹ region is shown in Figure 1, with the characteristic frequency values and spectral assignments of these bands given in Table 1.

Multivariate analysis with PCA-LDA was carried out on cells treated with increasing concentrations of the fungicides carbendazim and flusilazole over the concentration range 0.05-5 nM. One-dimensional (1-D) PCA-LDA scores plots and corresponding cluster vector plots representing the major biochemical alterations for cells treated with carbendazim are shown in Figures 2A and 2B respectively. Scores and cluster vector plots for cells treated with flusilazole are shown in Figures 3A and 3B respectively. It is clear from the scores plots in Figures 2A and 3A that cells treated with all concentrations of both carbendazim and flusilazole segregate away from the vehicle control along LD1; this was confirmed by one-way ANOVA followed by Tukey's post-hoc comparison tests, which revealed that the scores generated from PCA-LDA were significantly different from those of the vehicle control (Carbendazim: One-way ANOVA: $F_{5,48}$ = 8.63, P <0.0001; Tukey's post-hoc tests: P <0.01 for all concentrations; Flusilazole: $F_{5,48}$ = 7.12, P <0.0001; Tukey's post-hoc tests: P <0.01 for all concentrations). However, no significant differences were found between individual concentrations for either test agent (Tukey's multiple comparison test, P >0.05).

The cluster vector plot for carbendazim shown in Figure 2B revealed that the main wavenumbers associated with the segregation were very similar for each concentration. All concentrations tested revealed alterations in regions associated with C=O stretching and CH$_2$ bending of lipids (1744 and 1454 cm^{-1} respectively), as well as significant contributions from the Amide II protein region. Alterations induced by particular concentrations included those associated with the anti-parallel β-sheet conformation of Amide I and the base region (5 nM and 0.5 nM respectively, Table 2).

Cells treated with flusilazole showed some similarities to those treated with carbendazim in the cluster vector plot; however, regions associated with the Amide I and II region of proteins were more dominant (see Fig. 3B). Wavenumbers associated with the

Amide I and II regions of proteins (1663 and 1562 cm^{-1}) were identified as common to all concentrations tested; however, there was a greater variability in the other segregating wavenumbers between concentrations in comparison to cells treated with carbendazim, with some concentrations also associated with C=O stretching of lipids (0.5 nM) and fatty acids (0.05, 0.5, 1, and 5 nM, Table 2).

Comparison of cells treated with carbendazim *vs*. cells treated with flusilazole

As no significant differences were found between the individual concentrations of flusilazole and carbendazim, direct comparisons between these two agents were assessed by compiling spectra of all concentrations of the data. After subtraction of the vehicle control spectra, spectra of flusilazole and carbendazim-exposed cells were compared using cross-validated PCA-LDA followed by two sample *t*-test to assess the significance of the resulting scores, with the finding that cells treated with flusilazole were significantly different to those treated with carbendazim (see Fig. 4A). The cluster vector plot shown in Figure 4B denotes where these differences were most apparent, with the seven most segregating wavenumbers in regions associated with C=C stretching of lipids and fatty acids (1755 cm^{-1}), nucleic acids (1690 cm^{-1}), proteins (1477, 1562, 1601 cm^{-1}) and glycogen (1018 cm^{-1}), shown in Table 3.

As well as PCA-LDA, FFS was also used as a technique to identify discriminating wavenumbers. The high classification rate (~97%) generated by FFS is shown in Figure 4C, and the FSH with key discriminating wavenumbers marked is shown in Figure 4D. Wavenumbers responsible for the segregation of cells treated with flusilazole from those treated with carbendazim were also associated with lipid/fatty acid regions (1782, 1705, 1474 cm^{-1}), with some protein contribution (Amide III) and again significant contribution from carbohydrates/glycogen (1126, 1049 cm^{-1}; see Table 3).

Comparison of binary mixtures with single treatments

Cells were also treated with a mixture of carbendazim and flusilazole in the following combinations 0.05 nM carbendazim + 0.05 nM flusilazole; 0.05 nM carbendazim + 5 nM flusilazole; 5 nM carbendazim + 0.05 nM flusilazole; and 5 nM carbendazim + 5 nM flusilazole to determine if this generated any different alterations detectable by ATR-FTIR spectroscopy. All treatment combinations segregated significantly away from the control (see supplementary information Figs. S1A-D). Cluster vectors of cells treated with 0.05 nM and 5 nM of either carbendazim or flusilazole are shown in Figure 5A and 5B respectively for comparison with mixtures of these agents in different combinations (shown in Figs. 5C-5F, with wavenumber assignments in Table 4). Comparison of the single agent cluster vectors and the binary mixture cluster vectors reveals some similarities and some differences. With the binary mixtures, again there was a dominance of lipid and protein alterations, as seen with the single treatments. However, the alterations in the phospholipid region (~1750-1730 cm^{-1}) induced by the binary mixtures indicated a more pronounced effect in comparison to the single agent treatments, which was consistently seen for all treatment combinations.

Other parts of the spectrum were also highlighted as contributing towards the segregation in cells treated with binary mixtures, including those associated with DNA (1057, 1080 and 964 cm^{-1}). The peak at 1169 cm^{-1} (asymmetric stretching of CO-O-C in carbohydrates) was highlighted as a wavenumber consistently associated with treatment with binary mixtures in 3 out of 4 treatment combinations (Figs. 5C, 5D and 5F). From the cluster vectors plot of cells treated with single concentrations of flusilazole (Fig. 5B), there is also a small peak at 1169 cm^{-1}, which becomes more prominent and is highlighted by the peak detector when the agents are combined in a binary mixture, suggesting that when in combination there is a greater effect in this region.

Discussion

This study determined the application of ATR-FTIR spectroscopy coupled with multivariate feature extraction techniques in assessing the effects of environmentally-relevant concentrations of two differently acting agricultural fungicides in an amphibian cell line. The results confirmed distinct differences in cellular constituents treated with flusilazole or carbendazim, as may be expected from agents with different molecular targets (Derenne et al., 2011; Derenne et al., 2012). Cells treated with all concentrations of either flusilazole or carbendazim segregated significantly away from the vehicle control, demonstrating that ATR-FTIR spectroscopy is a sensitive technique capable of detecting cellular alterations even at very low concentrations, as has been recorded with other test agents (Johnson et al., 2014; Llabjani et al., 2011; Ukpebor et al., 2011). This result is significant as the concentration range used for each test agent was similar to that found in the aquatic environment (Chatupote and Panapitukkul, 2005; Palma et al., 2004) including areas in which amphibians are typically present (Strong et al., 2016). These results suggest that the combination of IR spectroscopy and chemometric analysis with the A6 cell line could serve as a useful model in identifying agents that might threaten amphibian health; however, extrapolation from the cellular to the whole organism and population level needs to be interpreted with caution, as there are differences in how chemical interact with whole organisms in comparison to individual cells (Schirmer, 2006).

IR spectroscopy, as well as being able to detect differences between control and treated cell populations in a rapid and high-throughput manner, provides detailed information about how particular agents affect cellular biochemistry through interpretation of the generated IR spectra (Jamin et al., 1998; Movasaghi et al., 2008). The use of chemometric methods such as PCA-LDA allows key features of the IR spectrum to be extracted in the

form of loadings and cluster vectors; the largest values corresponding to the most important wavenumbers responsible for segregation between control and treated cells, and can thus be considered biomarkers (Llabjani et al., 2010; Martin et al., 2010; Trevisan et al., 2012). Cells exposed to carbendazim exhibited alterations in regions associated with C=O stretching and CH_2 bending of lipids, with some protein contributions, indicative of a significant effect on cell membranes including the phospholipid bilayer. Lipids and Amide proteins are principally associated with the outer cell membrane, and the large spectral alterations seen in these regions are suggestive of disruption to membrane structure and integrity, indicative of lipid peroxidation (Gasper et al., 2009; Riding et al., 2012a). Lipid peroxidation is the initial step in damage to cell membranes caused by pesticides and other contaminants following the generation of reactive oxygen species (ROS) (Costa et al., 2008), and may be detectable using FTIR due to changes in the band assigned as C=O stretching of lipids at ~ 1740 cm^{-1} (Lamba et al., 1994; Riding et al., 2012a; Riding et al., 2012b), as seen here. The generation of ROS by environmental contaminants and subsequent oxidative damage may negatively affect tadpole reproduction and development and is related to amphibian population declines (Costa et al., 2008); therefore, there may be population-level consequences of these low-dose exposures. Carbendazim has previously been associated with lipid peroxidation in milk fish (Palanikumar et al., 2014) and in rats (Rajeswary et al., 2007), although only developmental and genotoxic effects have been measured thus far in amphibians (Yoon et al., 2008; Zoll-Moreux and Ferrier, 1999), despite the wide usage and detection of carbendazim in surface waters at low concentrations (Palma et al., 2004).

With flusilazole, the effects elicited in cells were mainly in the regions associated with Amide I and II proteins, with some lipid contribution. This again may be related to the cellular membranes as the functional properties of the plasma membrane are determined principally by the orientation of proteins within the membranes, which are readily detected by

IR spectroscopy (Gasper et al., 2009; Kong and Yu, 2007; Naumann, 2001). Flusilazole, like other triazole fungicides acts by interrupting the formation of fungal cell walls through inhibition of sterol-14α-demethylase (CYP51), which is highly conserved across taxa including animals, where it is utilised in the pathway to cholesterol formation; thus effects on cell membranes may not be restricted to the target species (Bossche et al., 1995; Zarn et al., 2003). The hazards posed by triazoles to wildlife is because their effects may not be limited to CYP51, and there is emerging evidence that they may accumulate in the tissues of amphibians, (Hansen et al., 2014; Poulsen et al., 2015; Smalling et al., 2013), although this may vary depending on the levels found in the environment (Smalling et al., 2015). At low levels of exposure, triazole fungicides have been associated with endocrine disruption, disrupting steroidogenesis in adult male frogs at concentrations as low as 1 µg/L (Poulsen et al., 2015), as well as developmental defects in tadpoles and embryos (Bernabò et al., 2016; Di Renzo et al., 2011; Groppelli et al., 2005; Papis et al., 2006). The changes in IR spectra elicited by flusilazole at similarly low concentrations in this study suggest that triazole fungicides are capable of generating responses in non-target organisms at environmentally-relevant concentrations. The possible endocrine disrupting effects of triazole fungicides have the potential to elicit population-level effects in amphibians by affecting sex ratios and disrupting normal reproductive behaviour (Kloas and Lutz, 2006).

High concentrations of agrichemicals are not typically measured in environmental compartments and instead much lower concentrations, often in complex mixtures tend to be detected, therefore amphibians are likely to be exposed to multiple agents in the environment (Khamis and Heikkila, 2013; Relyea, 2009; Smalling et al., 2015). Thus, in order to represent a more environmentally-realistic scenario, cells were also exposed to binary mixtures of flusilazole and carbendazim. Results from the cluster vector plots demonstrated a dominance of lipid and protein alterations, as seen with the single treatments; however, the alterations in

the phospholipid region (~1730-40 cm^{-1}) induced by the binary mixtures indicated a more pronounced effect in comparison to the single agent treatments, which was consistently seen for all treatment combinations, suggestive of further effects on the lipid bilayer when flusilazole and carbendazim were combined (Gasper et al., 2009). Other parts of the spectrum were also highlighted as contributing towards the segregation in cells treated with binary mixtures, including those associated with DNA (1057, 1080 and 964 cm^{-1}). Although carbendazim is not a direct-acting DNA damaging agent, it is a mitotic spindle poison and aneuploidogen which may secondarily affect DNA synthesis through the blocking of nuclear division (Davidse, 1986; McCarroll et al., 2002) and has been previously associated with genotoxicity in *X. laevis* tadpoles, although at higher concentrations than those used here (Zoll-Moreux and Ferrier, 1999). Instability of cell membranes may make cells more susceptible to further damage (Georgopapadakou, 1998; Lorito et al., 1996). As the phospholipid region of the spectrum showed consistent alterations following exposure to all mixtures, this suggests lipid peroxidation (Lamba et al., 1994; Riding et al., 2012a; Riding et al., 2012b). If this was indeed the case, the effects induced in other areas of the spectrum associated with DNA and carbohydrates could be caused indirectly by the products generated following the oxidation of lipids within the cell membrane (Burcham, 1998; Riding et al., 2012b); if the two agents are acting together and destabilising cell membranes the effects seen on other parts on the spectrum may be more pronounced.

Conclusions

- Amphibians are at risk of exposure to pesticides in the environment and there is emerging evidence that certain fungicides may accumulate in tissues, causing deleterious effects at low levels of exposure.

- This study presents the use of ATR-FTIR spectroscopy coupled with multivariate analysis to detect changes induced by environmentally-relevant concentrations of two mechanistically distinct fungicides in an amphibian cell line, both singly and in binary mixtures.

- Results suggested effects on cell membranes, as determined by alterations in the lipid and protein regions of the IR spectrum likely to be as a result of lipid peroxidation.

- Binary mixtures of flusilazole and carbendazim demonstrated consistent effects on areas of the spectrum associated with lipids, with alterations to other cell constituents including DNA also noted, suggestive of destabilisation of cell membranes, thus allowing further damage to subcellular moieties.

- Future work could aim to determine the effects of other common water constituents, such as nitrate/phosphate and metal ions in cell culture with these agents. Amphibians are known to be exposed to multiple stressors in the environment and creation of a more environmentally realistic scenario is key to understanding the effects at a cellular level.

References

Baker, M.J., Trevisan, J., Bassan, P., Bhargava, R., Butler, H.J., Dorling, K.M., Fielden, P.R., Fogarty, S.W., Fullwood, N.J., Heys, K.A., Hughes, C., Lasch, P., Martin-Hirsch, P.L., Obinaju, B., Sockalingum, G.D., Sulé-Suso, J., Strong, R.J., Walsh, M.J., Wood, B.R., Gardner, P., Martin, F.L., 2014. Using Fourier transform IR spectroscopy to analyze biological materials. Nature Protocols 9, 1771-1791.

Belden, J., McMurry, S., Smith, L., Reilley, P., 2010. Acute toxicity of fungicide formulations to amphibians at environmentally relevant concentrations. Environmental Toxicology and Chemistry 29, 2477-2480.

Berg, D., Büchel, K.H., Plempel, M., Zywietz, A., 1986. Action mechanisms of cell-division-arresting benzimidazoles and of sterol biosynthesis-inhibiting imidazoles, 1, 2, 4-triazoles, and pyrimidines. Mycoses 29, 221-229.

Bernabò, I., Guardia, A., Macirella, R., Sesti, S., Crescente, A., Brunelli, E., 2016. Effects of long-term exposure to two fungicides, pyrimethanil and tebuconazole, on survival and life history traits of Italian tree frog (*Hyla intermedia*). Aquatic Toxicology 172, 56-66.

Bjerregaard, H., 2007. Effects of cadmium on differentiation and cell cycle progression in cultured *Xenopus* kidney distal epithelial (A6) cells. Alternatives to Laboratory Animals: ATLA 35, 343-348.

Bjerregaard, H.F., Staermose, S., Vang, J., 2001. Effect of linear alkylbenzene sulfonate (LAS) on ion transport and intracellular calcium in kidney distal epithelial cells (A6). Toxicology in Vitro 15, 531-537.

Bossche, H.V., Koymans, L., Moereels, H., 1995. P450 inhibitors of use in medical treatment: Focus on mechanisms of action. Pharmacology & Therapeutics 67, 79-100.

Burcham, P.C., 1998. Genotoxic lipid peroxidation products: their DNA damaging properties and role in formation of endogenous DNA adducts. Mutagenesis 13, 287-305.

Chatupote, W., Panapitukkul, N., 2005. Regional assessment of nutrient and pesticide leaching in the vegetable production area of Rattaphum Catchment, Thailand. Water, Air, & Soil Pollution: Focus 5, 165-173.

Costa, M.J., Monteiro, D.A., Oliveira-Neto, A.L., Rantin, F.T., Kalinin, A.L., 2008. Oxidative stress biomarkers and heart function in bullfrog tadpoles exposed to Roundup Original®. Ecotoxicology 17, 153-163.

Darasch, S., Mosser, D.D., Bols, N.C., Heikkila, J.J., 1988. Heat shock gene expression in *Xenopus laevis* A6 cells in response to heat shock and sodium arsenite treatments. Biochemistry and Cell Biology 66, 862-870.

Davidse, L.C., 1986. Benzimidazole fungicides: mechanism of action and biological impact. Annual Review of Phytopathology 24, 43-65.

Derenne, A., Gasper, R., Goormaghtigh, E., 2011. The FTIR spectrum of prostate cancer cells allows the classification of anticancer drugs according to their mode of action. Analyst 136, 1134-1141.

Derenne, A., Verdonck, M., Goormaghtigh, E., 2012. The effect of anticancer drugs on seven cell lines monitored by FTIR spectroscopy. Analyst 137, 3255-3264.

Di Renzo, F., Bacchetta, R., Bizzo, A., Giavini, E., Menegola, E., 2011. Is the amphibian *X. laevis* WEC a good alternative method to rodent WEC teratogenicity assay? The example of the three triazole derivative fungicides Triadimefon, Tebuconazole, Cyproconazole. Reproductive Toxicology 32, 220-226.

Ellis, D.I., Goodacre, R., 2006. Metabolic fingerprinting in disease diagnosis: biomedical applications of infrared and Raman spectroscopy. Analyst 131, 875-885.

Faurskov, B., Bjerregaard, H.F., 1997. Effect of cadmium on active ion transport and cytotoxicity in cultured renal epithelial cells (A6). Toxicology in Vitro 11, 717-722.

Faurskov, B., Bjerregaard, H.F., 2000. Chloride secretion in kidney distal epithelial cells (A6) evoked by cadmium. Toxicology and Applied Pharmacology 163, 267-278.

Faurskov, B., Bjerregaard, H.F., 2002. Evidence for cadmium mobilization of intracellular calcium through a divalent cation receptor in renal distal epithelial A6 cells. Pflügers Archiv 445, 40-50.

Fent, K., 2001. Fish cell lines as versatile tools in ecotoxicology: assessment of cytotoxicity, cytochrome P4501A induction potential and estrogenic activity of chemicals and environmental samples. Toxicology in Vitro 15, 477-488.

Gasper, R., Dewelle, J., Kiss, R., Mijatovic, T., Goormaghtigh, E., 2009. IR spectroscopy as a new tool for evidencing antitumor drug signatures. Biochimica et Biophysica Acta (BBA) - Biomembranes 1788, 1263-1270.

Georgopapadakou, N.H., 1998. Antifungals: mechanism of action and resistance, established and novel drugs. Current Opinion in Microbiology 1, 547-557.

Gorrochategui E, Lacorte S, Tauler R, Martin FL. 2016. Perfluoroalkylated Substance Effects in Xenopus laevis A6 Kidney Epithelial Cells Determined by ATR-FTIR Spectroscopy and Chemometric Analysis. Chemical Research in Toxicology 29, 924-932

Groppelli, S., Pennati, R., De Bernardi, F., Menegola, E., Giavini, E., Sotgia, C., 2005. Teratogenic effects of two antifungal triazoles, triadimefon and triadimenol, on *Xenopus laevis* development: Craniofacial defects. Aquatic Toxicology 73, 370-381.

Hanlon, S.M., Parris, M.J., 2014. The interactive effects of chytrid fungus, pesticides, and exposure timing on gray treefrog (Hyla versicolor) larvae. Environmental Toxicology and Chemistry 33, 216-222.

Hansen, M., Poulsen, R., Luong, X., Sedlak, D.L., Hayes, T., 2014. Liquid chromatography tandem mass spectrometry method using solid-phase extraction and bead-beating-assisted matrix solid-phase

dispersion to quantify the fungicide tebuconazole in controlled frog exposure study: analysis of water and animal tissue. Analytical and Bioanalytical Chemistry 406, 7677-7685.

Hayes, T.B., Case, P., Chui, S., Chung, D., Haeffele, C., Haston, K., Lee, M., Mai, V.P., Marjuoa, Y., Parker, J., Tsui, M., 2006. Pesticide mixtures, endocrine disruption, and amphibian declines: Are we underestimating the impact? Environmental Health Perspectives 114, 40-50.

Heikkila, J.J., Darasch, S.P., Mosser, D.D., Bols, N.C., 1987. Heat and sodium arsenite act synergistically on the induction of heat shock gene expression in *Xenopus laevis* A6 cells. Biochemistry and Cell Biology 65, 310-316.

Heys, K.A., Riding, M.J., Strong, R.J., Shore, R.F., Pereira, M.G., Jones, K.C., Semple, K.T., Martin, F.L., 2014. Mid-infrared spectroscopic assessment of nanotoxicity in Gram-negative vs. Gram-positive bacteria. Analyst 139, 896-905.

Holman, H.-Y.N., Goth-Goldstein, R., Blakely, E.A., Bjornstad, K., Martin, M.C., McKinney, W.R., 2000a. Individual human cell responses to low doses of chemicals studied by synchrotron infrared spectromicroscopy. BiOS 2000 The International Symposium on Biomedical Optics, 57-63.

Holman, H.-Y.N., Goth-Goldstein, R., Martin, M.C., Russell, M.L., McKinney, W.R., 2000b. Low-dose responses to 2, 3, 7, 8-tetrachlorodibenzo-p-dioxin in single living human cells measured by synchrotron infrared spectromicroscopy. Environmental Science & Technology 34, 2513-2517.

Houlahan, J.E., Findlay, C.S., Schmidt, B.R., Meyer, A.H., Kuzmin, S.L., 2000. Quantitative evidence for global amphibian population declines. Nature 404, 752-755.

Hua, J., Relyea, R., 2014. Chemical cocktails in aquatic systems: Pesticide effects on the response and recovery of >20 animal taxa. Environmental Pollution 189, 18-26.

Jamin, N., Dumas, P., Moncuit, J., Fridman, W.-H., Teillaud, J.-L., Carr, G.L., Williams, G.P., 1998. Highly resolved chemical imaging of living cells by using synchrotron infrared microspectrometry. Proceedings of the National Academy of Sciences 95, 4837-4840.

Johnson, C.M., Pleshko, N., Achary, M., Suri, R.P.S., 2014. Rapid and sensitive screening of 17β-estradiol estrogenicity using Fourier transform infrared imaging spectroscopy (FT-IRIS). Environmental Science & Technology 48, 4581-4587.

Kelly, J.G., Trevisan, J.l., Scott, A.D., Carmichael, P.L., Pollock, H.M., Martin-Hirsch, P.L., Martin, F.L., 2011. Biospectroscopy to metabolically profile biomolecular structure: a multistage approach linking computational analysis with biomarkers. Journal of Proteome Research 10, 1437-1448.

Khamis, I., Heikkila, J.J., 2013. Enhanced HSP30 and HSP70 accumulation in *Xenopus* cells subjected to concurrent sodium arsenite and cadmium chloride stress. Comparative Biochemistry and Physiology Part C: Toxicology & Pharmacology 158, 165-172.

Kloas, W., Lutz, I., 2006. Amphibians as model to study endocrine disrupters. Journal of chromatography A 1130, 16-27.

Kong, J., Yu, S., 2007. Fourier transform infrared spectroscopic analysis of protein secondary structures. Acta Biochimica et Biophysica Sinica 39, 549-559.

Lamba, O.P., Borchman, D., Garner, W.H., 1994. Spectral characterization of lipid peroxidation in rabbit lens membranes induced by hydrogen peroxide in the presence of Fe2+ Fe3+ cations: A site-specific catalyzed oxidation. Free Radical Biology and Medicine 16, 591-601.

Llabjani, V., Trevisan, J., Jones, K.C., Shore, R.F., Martin, F.L., 2010. Binary mixture effects by PBDE congeners (47, 153, 183, or 209) and PCB congeners (126 or 153) in MCF-7 cells: Biochemical alterations assessed by IR spectroscopy and multivariate analysis. Environmental Science & Technology 44, 3992-3998.

Llabjani, V., Trevisan, J., Jones, K.C., Shore, R.F., Martin, F.L., 2011. Derivation by infrared spectroscopy with multivariate analysis of bimodal contaminant-induced dose-response effects in MCF-7 cells. Environmental Science & Technology 45, 6129-6135.

Lorito, M., Woo, S.L., D'Ambrosio, M., Harman, G.E., Hayes, C.K., Kubicek, C.P., Scala, F., 1996. Synergistic interaction between cell wall degrading enzymes and membrane affecting compounds. MPMI-Molecular Plant Microbe Interactions 9, 206-213.

Mann, R., Hyne, R., Choung, C., Wilson, S., 2009. Amphibians and agricultural chemicals: Review of the risks in a complex environment. Environmental Pollution 157, 2903-2927.

Martin, F.L., Kelly, J.G., Llabjani, V., Martin-Hirsch, P.L., Patel, I.I., Trevisan, J., Fullwood, N.J., Walsh, M.J., 2010. Distinguishing cell types or populations based on the computational analysis of their infrared spectra. Nature Protocols 5, 1748-1760.

McCarroll, N.E., Protzel, A., Ioannou, Y., Frank Stack, H., Jackson, M.A., Waters, M.D., Dearfield, K.L., 2002. A survey of EPA/OPP and open literature on selected pesticide chemicals: III. Mutagenicity and carcinogenicity of benomyl and carbendazim. Mutation Research/Reviews in Mutation Research 512, 1-35.

McMullen, M., Bergstrom, G., De Wolf, E., Dill-Macky, R., Hershman, D., Shaner, G., Van Sanford, D., 2012. A Unified Effort to Fight an Enemy of Wheat and Barley: Fusarium Head Blight. Plant Disease 96, 1712-1728.

Mecozzi, M., Pietroletti, M., Di Mento, R., 2007. Application of FTIR spectroscopy in ecotoxicological studies supported by multivariate analysis and 2D correlation spectroscopy. Vibrational Spectroscopy 44, 228-235.

Movasaghi, Z., Rehman, S., ur Rehman, D.I., 2008. Fourier transform infrared (FTIR) spectroscopy of biological tissues. Applied Spectroscopy Reviews 43, 134-179.

Music, E., Khan, S., Khamis, I., Heikkila, J.J., 2014. Accumulation of heme oxygenase-1 (HSP32) in *Xenopus laevis* A6 kidney epithelial cells treated with sodium arsenite, cadmium chloride or proteasomal inhibitors. Comparative Biochemistry and Physiology Part C: Toxicology & Pharmacology 166, 75-87.

Naumann, D., 2001. FT-infrared and FT-Raman spectroscopy in biomedical research. Applied Spectroscopy Reviews 36, 239-298.

Palanikumar, L., Kumaraguru, A.K., Ramakritinan, C.M., Anand, M., 2014. Toxicity, biochemical and clastogenic response of chlorpyrifos and carbendazim in milkfish *Chanos chanos*. International Journal of Environmental Science and Technology 11, 765-774.

Palma, G., Śnchez, A., Olave, Y., Encina, F., Palma, R., Barra, R., 2004. Pesticide levels in surface waters in an agricultural-forestry basin in Southern Chile. Chemosphere 57, 763-770.

Papis, E., Bernardini, G., Gornati, R., Prati, M., 2006. Triadimefon causes branchial arch malformations in *Xenopus laevis* embryos (5 pp). Environmental Science and Pollution Research 13, 251-255.

Poulsen, R., Luong, X., Hansen, M., Styrishave, B., Hayes, T., 2015. Tebuconazole disrupts steroidogenesis in *Xenopus laevis*. Aquatic Toxicology 168, 28-37.

Quaranta, A., Bellantuono, V., Cassano, G., Lippe, C., 2009. Why amphibians are more sensitive than mammals to xenobiotics. PLoS One 4, e7699.

Rajeswary, S., Kumaran, B., Ilangovan, R., Yuvaraj, S., Sridhar, M., Venkataraman, P., Srinivasan, N., Aruldhas, M.M., 2007. Modulation of antioxidant defense system by the environmental fungicide carbendazim in Leydig cells of rats. Reproductive Toxicology 24, 371-380.

Relyea, R.A., 2009. A cocktail of contaminants: how mixtures of pesticides at low concentrations affect aquatic communities. Oecologia 159, 363-376.

Riding, M.J., Martin, F.L., Trevisan, J., Llabjani, V., Patel, I.I., Jones, K.C., Semple, K.T., 2012a. Concentration-dependent effects of carbon nanoparticles in gram-negative bacteria determined by infrared spectroscopy with multivariate analysis. Environmental Pollution 163, 226-234.

Riding, M.J., Trevisan, J., Hirschmugl, C.J., Jones, K.C., Semple, K.T., Martin, F.L., 2012b. Mechanistic insights into nanotoxicity determined by synchrotron radiation-based Fourier-transform infrared imaging and multivariate analysis. Environment International 50, 56-65.

Schirmer, K., 2006. Proposal to improve vertebrate cell cultures to establish them as substitutes for the regulatory testing of chemicals and effluents using fish. Toxicology 224, 163-183.

Scholz, S., Sela, E., Blaha, L., Braunbeck, T., Galay-Burgos, M., García-Franco, M., Guinea, J., Klüver, N., Schirmer, K., Tanneberger, K., Tobor-Kapłon, M., Witters, H., Belanger, S., Benfenati, E., Creton, S., Cronin, M.T.D., Eggen, R.I.L., Embry, M., Ekman, D., Gourmelon, A., Halder, M., Hardy, B., Hartung, T., Hubesch, B., Jungmann, D., Lampi, M.A., Lee, L., Léonard, M., Küster, E., Lillicrap, A., Luckenbach, T., Murk, A.J., Navas, J.M., Peijnenburg, W., Repetto, G., Salinas, E., Schüürmann, G., Spielmann, H., Tollefsen, K.E., Walter-Rohde, S., Whale, G., Wheeler, J.R., Winter, M.J., 2013. A European perspective on alternatives to animal testing for environmental hazard identification and risk assessment. Regulatory Toxicology and Pharmacology 67, 506-530.

Smalling, K.L., Fellers, G.M., Kleeman, P.M., Kuivila, K.M., 2013. Accumulation of pesticides in pacific chorus frogs (*Pseudacris regilla*) from California's Sierra Nevada Mountains, USA. Environmental Toxicology and Chemistry 32, 2026-2034.

Smalling, K.L., Reeves, R., Muths, E., Vandever, M., Battaglin, W.A., Hladik, M.L., Pierce, C.L., 2015. Pesticide concentrations in frog tissue and wetland habitats in a landscape dominated by agriculture. Science of The Total Environment 502, 80-90.

Sparling, D.W., Fellers, G.M., McConnell, L.L., 2001. Pesticides and amphibian population declines in California, USA. Environmental Toxicology and Chemistry 20, 1591-1595.

Sparling, D.W., Linder, G., Bishop, C.A., Krest, S.K., 2010. Ecotoxicology of amphibians and reptiles.

Strong, R.J., Halsall, C.J., Ferenčík, M., Jones, K.C., Shore, R.F., Martin, F.L., 2016. Biospectroscopy reveals the effect of varying water quality on tadpole tissues of the common frog (*Rana temporaria*). Environmental Pollution 213, 322-337.

Stuart, S.N., Chanson, J.S., Cox, N.A., Young, B.E., Rodrigues, A.S.L., Fischman, D.L., Waller, R.W., 2004. Status and trends of amphibian declines and extinctions worldwide. Science 306, 1783-1786.

Thit, A., Selck, H., Bjerregaard, H.F., 2013. Toxicity of CuO nanoparticles and Cu ions to tight epithelial cells from *Xenopus laevis* (A6): Effects on proliferation, cell cycle progression and cell death. Toxicology in Vitro 27, 1596-1601.

Trevisan, J., Angelov, P.P., Carmichael, P.L., Scott, A.D., Martin, F.L., 2012. Extracting biological information with computational analysis of Fourier-transform infrared (FTIR) biospectroscopy datasets: current practices to future perspectives. Analyst 137, 3202-3215.

Trevisan, J., Angelov, P.P., Scott, A.D., Carmichael, P.L., Martin, F.L., 2013. IRootLab: a free and open-source MATLAB toolbox for vibrational biospectroscopy data analysis. Bioinformatics 29, 1095-1097.

Trevisan, J., Park, J., Angelov, P.P., Ahmadzai, A.A., Gajjar, K., Scott, A.D., Carmichael, P.L., Martin, F.L., 2014. Measuring similarity and improving stability in biomarker identification methods applied to Fourier-transform infrared (FTIR) spectroscopy. Journal of Biophotonics 7, 254-265.

Ukpebor, J., Llabjani, V., Martin, F.L., Halsall, C.J., 2011. Sublethal genotoxicity and cell alterations by organophosphorus pesticides in MCF-7 cells: Implications for environmentally relevant concentrations. Environmental Toxicology and Chemistry 30, 632-639.

Wolff, J., 2009. Plasma membrane tubulin. Biochimica et Biophysica Acta (BBA) - Biomembranes 1788, 1415-1433.

Woolfson, J.P., Heikkila, J.J., 2009. Examination of cadmium-induced expression of the small heat shock protein gene, hsp30, in *Xenopus laevis* A6 kidney epithelial cells. Comparative Biochemistry and Physiology Part A: Molecular & Integrative Physiology 152, 91-99.

Yoon, C.-S., Jin, J.-H., Park, J.-H., Youn, H.-J., Cheong, S.-W., 2003. The fungicide benomyl inhibits differentiation of neural tissue in the *Xenopus* embryo and animal cap explants. Environmental Toxicology 18, 327-337.

Yoon, C.S., Jin, J.H., Park, J.H., Yeo, C.Y., Kim, S.J., Hwang, Y.G., Hong, S.J., Cheong, S.W., 2008. Toxic effects of carbendazim and n-butyl isocyanate, metabolites of the fungicide benomyl, on early development in the African clawed frog, *Xenopus laevis*. Environmental Toxicology 23, 131-144.

Yu, L., Eaton, D.C., Helms, M.N., 2007. Effect of divalent heavy metals on epithelial Na+ channels in A6 cells. American Journal of Physiology-Renal Physiology 293, F236-F244.

Zarn, J.A., Brüschweiler, B.J., Schlatter, J.R., 2003. Azole fungicides affect mammalian steroidogenesis by inhibiting sterol 14 alpha-demethylase and aromatase. Environmental Health Perspectives 111, 255-261.

Zoll-Moreux, C., Ferrier, V., 1999. The Jaylet test (newt micronucleus test) and the micronucleus test in xenopus: Two in vivo tests on amphibia evaluation of the genotoxicity of five environmental pollutants and of five effluents. Water Research 33, 2301-2314.

Figure legends

Figure 1. Typical mean second derivative spectrum of untreated *Xenopus laevis* kidney epithelial (A6) cells in the 1800-900 cm^{-1} region following analysis with ATR-FTIR spectroscopy. Corresponding wavenumber assignments are shown in Table 1.

Figure 2. Cross-validated one-dimensional PCA-LDA scores plot (**A**) and corresponding cluster vectors plot (**B**) of A6 cells treated with increasing concentrations of carbendazim following analysis with ATR-FTIR spectroscopy. The vehicle control is set at the origin of the cluster vectors plot. Asterisks indicate a significant difference from the DMSO vehicle control (VC) at the $P <0.01$ level as determined by One-Way ANOVA followed by Tukey's post-hoc test carried out on averages of each experimental replicate ($n = 9$). Wavenumber assignments from cluster vector plots are shown in Table 2.

Figure 3. Cross-validated one-dimensional PCA-LDA scores plot (**A**) and corresponding cluster vectors plot (**B**) of A6 cells treated with increasing concentrations of flusilazole following analysis with ATR-FTIR spectroscopy. The vehicle control is set at the origin of the cluster vectors plot. Asterisks indicate a significant difference from the DMSO vehicle control (VC) at the $P <0.01$ level as determined by One-Way ANOVA followed by Tukey's post-hoc test carried out on averages of each experimental replicate ($n = 9$). Wavenumber assignments from cluster vector plots are shown in Table 2.

Figure 4. Cross-validated one-dimensional PCA-LDA scores plot **(A)** and corresponding cluster vectors plot **(B)** directly comparing cells treated with either carbendazim or flusilazole following analysis with ATR-FTIR spectroscopy. Flusilazole is set at the origin for direct comparison with carbendazim in the cluster vectors plot. For a comparison with PCA-LDA, Figures **C** and **D** show the classification of cells treated with either flusilazole or carbendazim into their respective categories and the feature histogram generated following forward feature selection respectively. Wavenumber assignments are shown in Table 3.

Figure 5. Cluster vectors plots generated from single treatments of A6 cells with carbendazim **(A)** and flusilazole **(B)** for comparison with loadings plots generated following treatment of A6 cells with binary mixtures of a combination of carbendazim and flusilazole at different concentrations **(C-F)**. Wavenumber assignments are shown in Table 4.
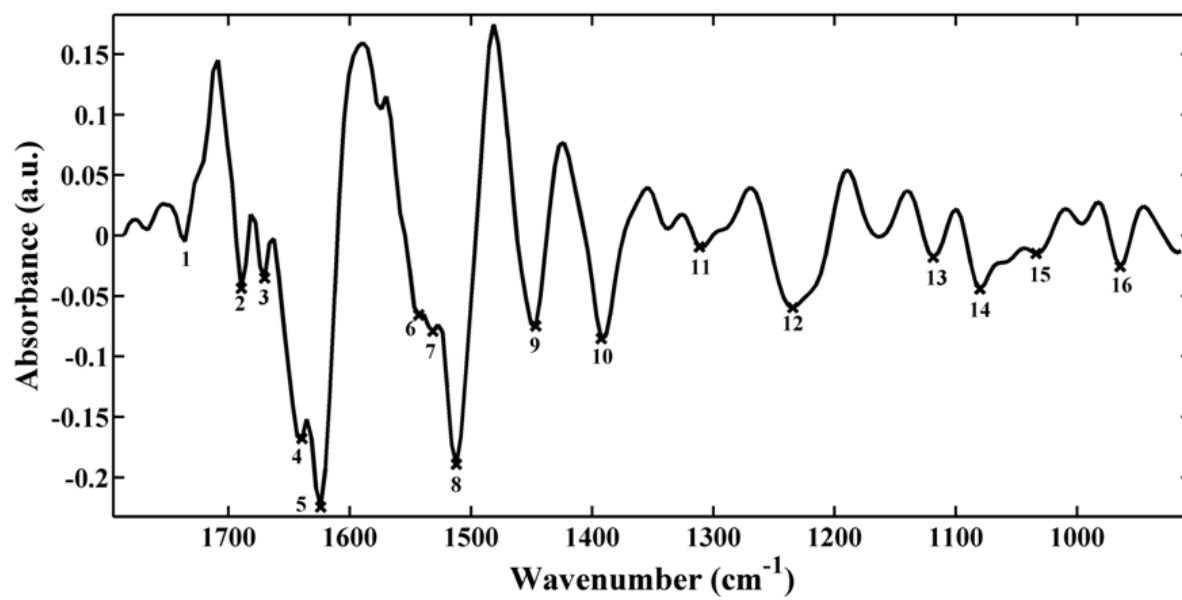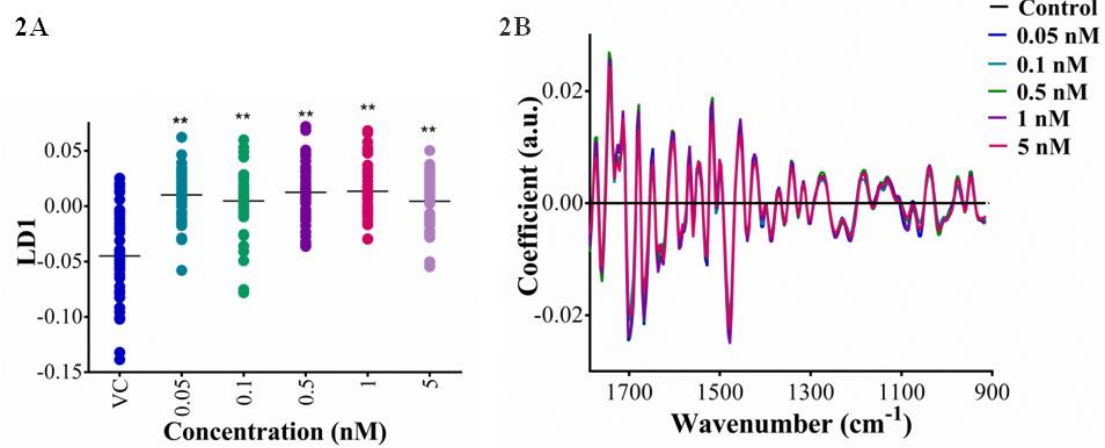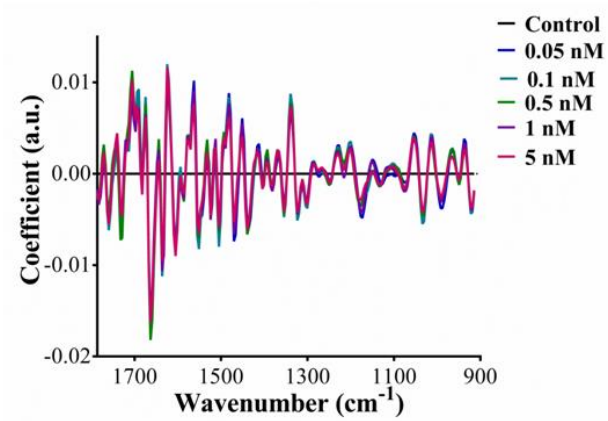
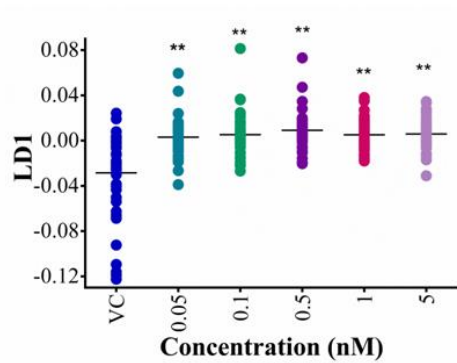**Figure 1.**
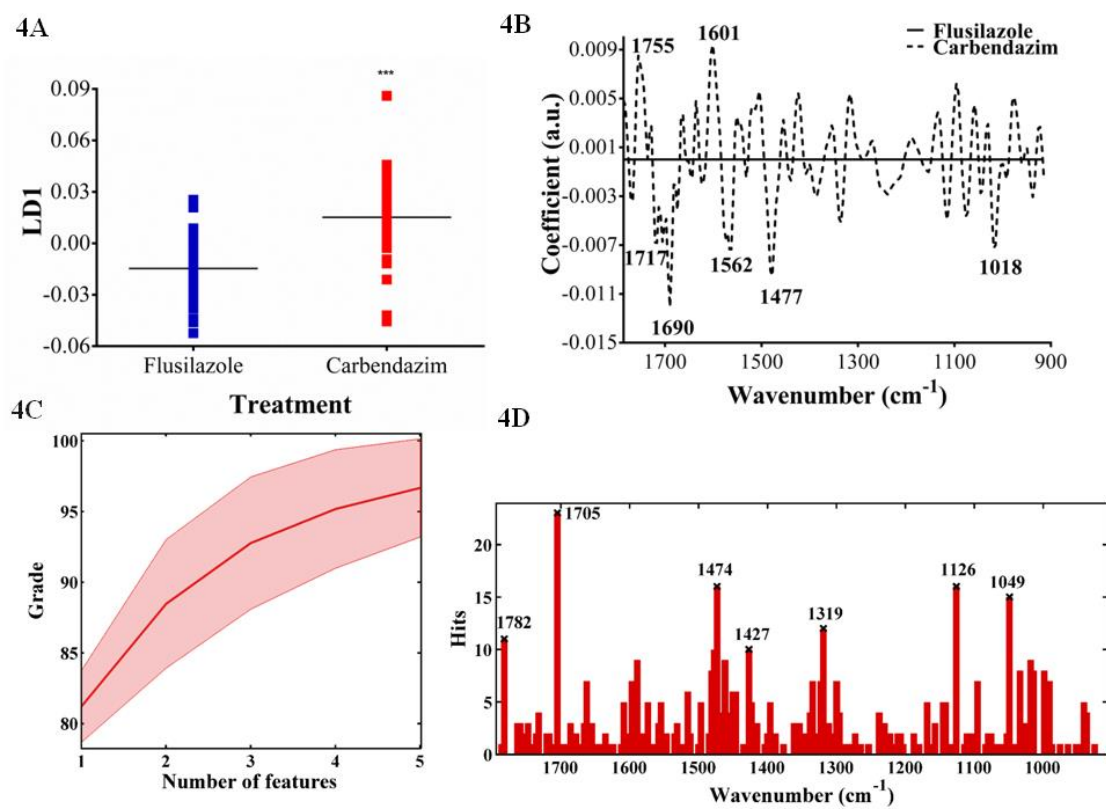
Figure 2.

Figure 3.
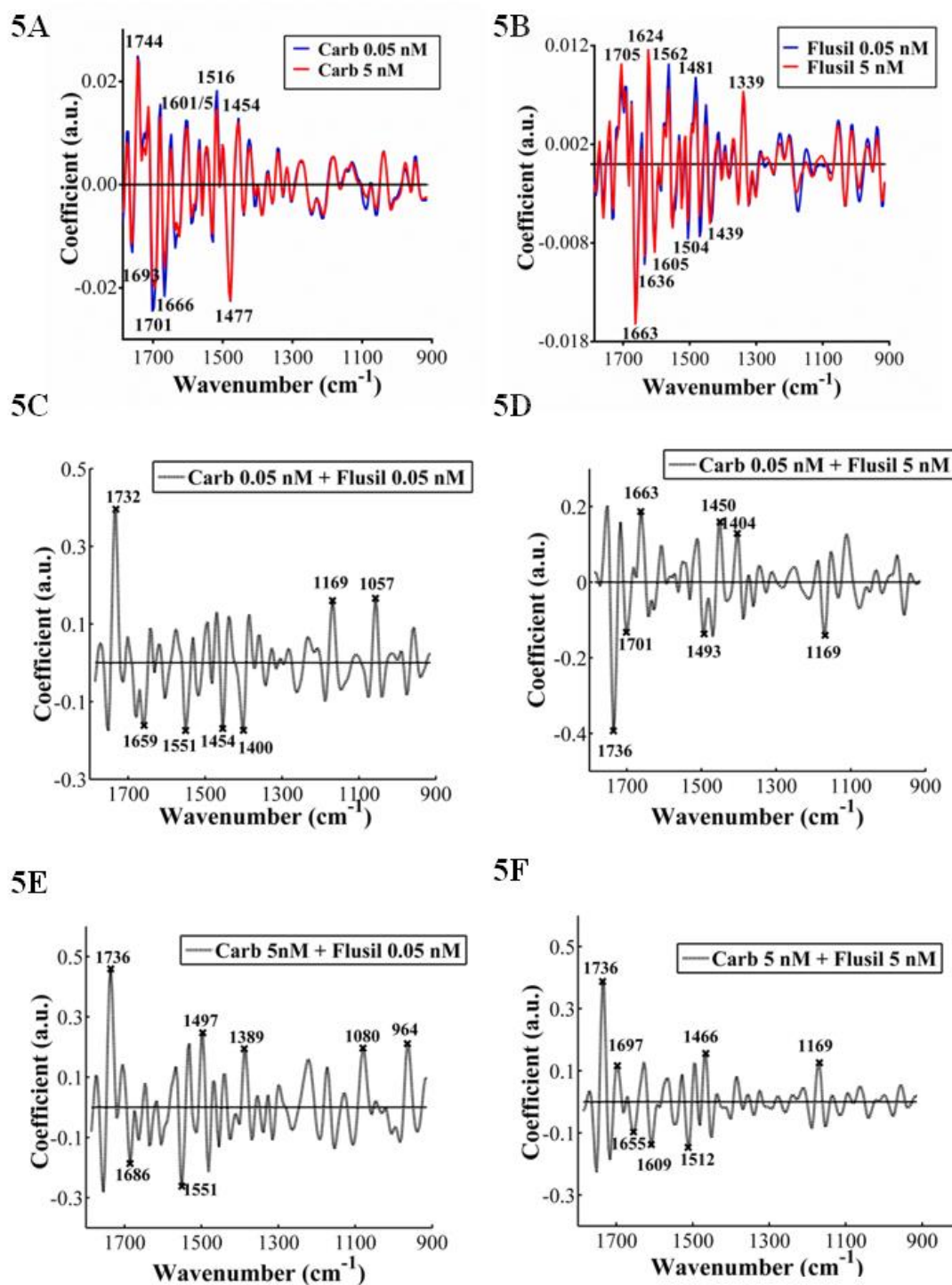
3A

Figure 4.

Figure 5.

Table 1. Band assignments of major absorptions in the second derivative IR spectra of untreated *Xenopus laevis* kidney epithelial (A6) cells in the 1800-900 cm^{-1} cell fingerprint region based on the literature. Sources: (Movasaghi et al., 2008; Naumann, 2001)

Peak Number	Wavenumber (cm^{-1})	Proposed Spectral Assignment
1	1736	C=O stretching of esters/phospholipids
2	1690	Peak of nucleic acids due to base carbonyl stretching and ring breathing mode
3	1670	Amide I (anti-parallel β-sheet)
4	1639	Amide I
5	1624	Amide I (β-sheet)
6	1543	Amide II (N-H bending, C-N stretching)
7	1531	Amide II
8	1512	CH bending from phenyl rings
9	1447	Asymmetric CH$_3$ bending of the methyl groups of proteins
10	1393	Symmetric CH$_3$ bending of the methyl groups of proteins
11	1312	Amide III
12	1234	Asymmetric phosphate stretching overlapped with amide III of proteins
13	1119	C-O stretching mode/deformations of carbohydrates
14	1080	Symmetric phosphate stretching
15	1034	Glycogen
16	964	C-O deoxyribose

Table 2. Distinguishing wavenumbers and proposed assignments generated from the cluster vector plots of A6 cells analysed with ATR-FTIR spectroscopy after treatment with increasing concentrations of either carbendazim or flusilazole. Sources: (Movasaghi et al., 2008; Naumann, 2001)

Treatment	Wavenumber (cm^{-1})	Tentative Assignment	Concentration (nM)
Carbendazim	1744	C=O stretching of phospholipids, triglycerides, cholesterol esters	All
	1701	Fatty acid esters	0.05, 0.1, 1
	1697	Base region	0.5
	1693	Anti-parallel β-sheet of Amide I	5
	1666	C=O stretching of pyrimidine bases	All
	1605	Amide I	0.05, 0.5, 1
	1601	C=N cytosine, N-H adenine	0.1, 5
	1516	Amide II	All
	1477	Proteins	All
	1454	CH$_2$ bending of lipids, with some contribution from proteins	All
Flusilazole	1732	C=O stretching (phospholipids)/fatty acid esters	0.5
	1705	Fatty acid esters	0.05, 0.5, 1, 5
	1690	Peak of nucleic acids due to base carbonyl stretching and ring breathing mode	0.1
	1663	Amide I	All
	1636	B-sheet structure of amide I	0.05, 0.5, 1
	1624	Amide I (β-sheet)	0.1, 5
	1605	Asymmetric stretch of polysaccharides/pectins	0.05, 0.5, 1
	1562	Amide II region	All
	1504	In-plane CH bending from phenyl rings	0.05, 0.1
	1481	Amide II	0.05, 0.1, 1, 5
	1439	Protein	5
	1339	In-plane C-O stretching vibration combined with the ring stretch of phenyl	0.1, 0.5, 1, 5

Table 3. Distinguishing wavenumbers and proposed assignments generated from cluster vectors and feature histograms following a direct comparison of A6 cells treated with either carbendazim or flusilazole after analysis with ATR-FTIR spectroscopy. Vehicle control spectra were first subtracted from treated spectra to directly compare the difference in alterations induced by each agent. All concentrations were combined as there were no significant differences between concentrations for each agent. Sources: (Movasaghi et al., 2008; Naumann, 2001)

Analysis Type	Wavenumber (cm^{-1})	Tentative Assignment
Cluster Vectors	1755	Stretching C=C, phospholipids fatty acids
	1717	C=O stretching of carbonic acid
	1690	Peak of nucleic acids due to base carbonyl stretching and ring breathing mode[1]
	1601	C=N cytosine, N-H adenine
	1562	Amide II
	1477	Proteins
	1018	Glycogen
Feature Histograms	1782	Fatty acid esters
	1705	Fatty acid esters
	1474	Protein/CH$_2$ bending of lipids
	1427	CH$_2$ bending
	1319	Amide III
	1126	C-O stretching, disaccharides/sucrose
	1049	Glycogen/carbohydrates

Table 4. Distinguishing wavenumbers and proposed assignments generated from loadings plots following treatment of A6 cells with binary mixtures of carbendazim and flusilazole after analysis with ATR-FTIR spectroscopy. Sources: (Movasaghi et al., 2008; Naumann, 2001).

Treatment	Wavenumber (cm^{-1})	Tentative Assignment
0.05 nM Carbendazim + 0.05 nM Flusilazole	1732	Fatty acid esters/C=O stretching of phospholipids
	1659	Amide I
	1551	Amide II
	1454	CH$_2$ bending of lipids, with some contribution from proteins
	1400	Symmetric stretching of methyl groups in proteins/COO$^-$ vibration of fatty acids
	1169	Asymmetric stretching of CO-O-C in carbohydrates
	1057	C-O-C stretching of nucleic acids and phospholipids
0.05 nM Carbendazim + 5 nM Flusilazole	1736	C=O stretching of phospholipids
	1701	Fatty acid esters
	1663	Amide I
	1493	In-plane CH bending vibration
	1450	Methylene deformation
	1404	CH$_3$ asymmetric deformation
	1169	Asymmetric stretching of CO-O-C in carbohydrates
5 nM Carbendazim + 0.05 nM Flusilazole	1736	C=O stretching of phospholipids
	1686	Amide I (disordered structure)
	1551	Amide II
	1497	C=C deformation, C-H
	1389	Stretching C-O, C-H deformation
	1080	Symmetric phosphate stretching
	964	C-O deoxyribose, C-C
5 nM Carbendazim + 5 nM Flusilazole	1736	C=O stretching of phospholipids
	1697	Base region
	1655	Amide I of proteins (α-helix)
	1609	Adenine vibration in DNA
	1512	CH bending from phenyl rings
	1466	CH$_2$ scissoring mode of the acyl chain of lipid
	1169	Asymmetric stretching of CO-O-C in carbohydrates

Electronic Supplementary Information

Infrared spectroscopy detects changes in an amphibian cell line induced by fungicides: comparison of single and mixture effects

Rebecca J. Strong[1], Crispin J. Halsall[1*], Kevin C. Jones[1], Richard F. Shore[2] and Francis L. Martin[1,3*]
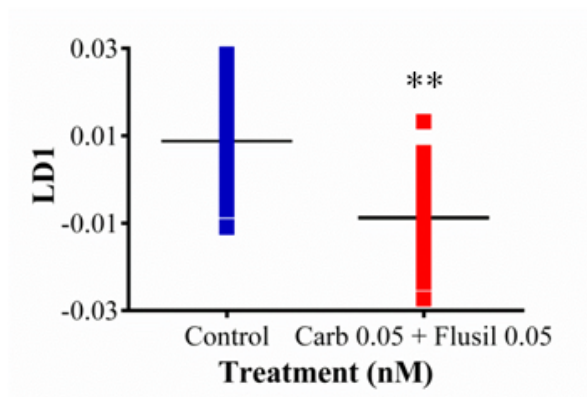
[1]*Lancaster Environment Centre, Lancaster University, Bailrigg, Lancaster LA1 4YQ, UK*

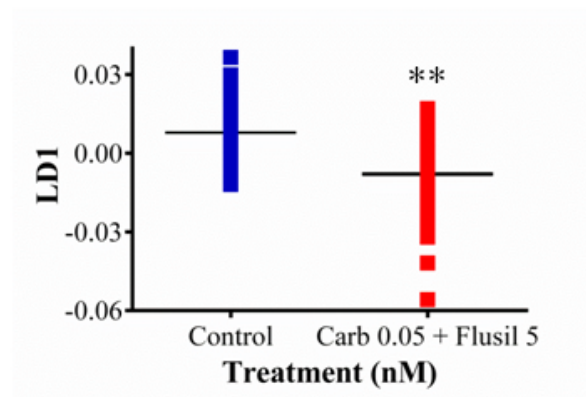[2] *Centre for Ecology and Hydrology, Lancaster University, Bailrigg, Lancaster LA1 4YQ, UK*

[3]*School of Pharmacy and Biomedical Sciences, University of Central Lancashire, Preston PR1 2HE, UK*

[*] **Corresponding authors.** Email address: c.halsall@lancaster.ac.uk (C.J. Halsall); f.martin@lancaster.ac.uk (F.L. Martin)
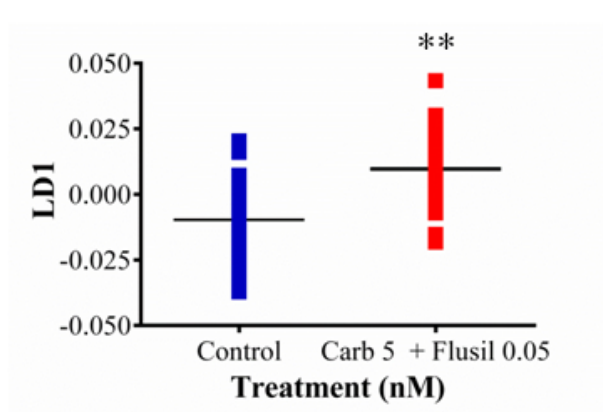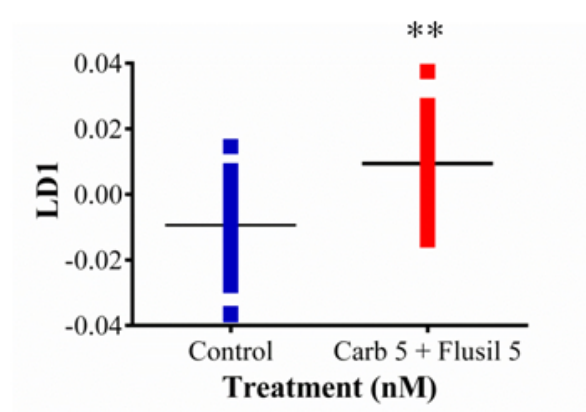
Figure S1. Cross-validated one-dimensional PCA-LDA scores plots of A6 cells treated with binary mixtures of flusilazole and carbendazim following analysis with ATR-FTIR spectroscopy. Asterisks indicate a significant difference from the vehicle control (DMSO) at the $P < 0.01$ level as determined by two-sample t-tests.